

# Compositeness of near-threshold $s$ -wave resonances

Tomona Kinugawa\* and Tetsuo Hyodo†

Department of Physics, Tokyo Metropolitan University, Hachioji 192-0397, Japan

(Dated: August 2, 2024)

The near-threshold clustering phenomenon is well understood by the low-energy universality, for shallow bound states below the threshold. Nevertheless, the characteristics of resonances slightly above the threshold still lack thorough elucidation. We introduce a novel probabilistic interpretation scheme for complex compositeness of resonances, in which resonances with unphysically large decay widths are inherently excluded. Employing this scheme to analyze resonances via the effective range expansion, we demonstrate that near-threshold resonances have small composite fraction, in sharp contrast to shallow bound states below the threshold.

*Introduction:* In nature, the hierarchical structure is formed by the particles in different energy scales, such as quarks, hadrons, nuclei, and atoms. In each hierarchy, the clustering phenomenon is known to emerge universally, leading to the formation of subunits which act as effective degrees of freedom. For example, while the fundamental degree of freedom in nuclear hierarchy is the nucleon, the  $^{12}\text{C}$  Hoyle state consists of three  $\alpha$  particles ( $^4\text{He}$  nuclei) as the subunits [1, 2]. In hadron physics, in addition to the ordinary hadrons composed of quarks as the fundamental particles, it is considered that loosely bound systems of hadrons, the hadronic molecules, manifest as alternative internal structures [3]. Such exotic internal structure of hadronic molecules has recently attracted a lot of attention from researchers [4, 5].

To quantitatively characterize the cluster structure of hadrons, the notion of compositeness has been introduced and subsequently developed [6–47]. The compositeness of a stable bound state refers to the probability of finding the composite component in the wave function. This concept has been utilized across the hierarchical structure to analyze the deuteron, hypertriton and  $^4\text{He}$  dimer [6, 37, 39, 42, 47]. The compositeness is also expected to be useful in quantitatively extracting the molecular component from the wave function of exotic hadrons which are the superposition of various components. However, the majority of exotic hadrons decay with finite lifetime. This instability leads to the complex-valued compositeness [14], posing challenges in interpretation. This is the first issue which we want to discuss in this paper.

Another remarkable fact about exotic hadrons is their appearance near the two-body threshold energy. Near-threshold phenomena follow the low-energy universality, regardless of the details of the system, particularly when the magnitude of the scattering length is sufficiently larger than other characteristic length scales of the system [48, 49]. Universality dictates that the near-threshold  $s$ -wave bound states below the threshold are typically composite dominant, indicating the clustering phenomena [18, 44, 50–53]. In contrast, the detailed properties of near-threshold  $s$ -wave resonances above the threshold have not been thoroughly studied. However,

recent analysis of the  $K^- \Lambda$  correlation function data for  $\Xi(1620)$  [54] suggests the existence of such a resonance. Furthermore,  $s$ -wave resonances can also be realized in the cold-atom physics via the Feshbach resonance induced by the external magnetic field [55]. Therefore, the second issue addressed in this paper is to study the nature of near-threshold  $s$ -wave resonances.

Our objective in this paper is to offer a plausible interpretation of the complex compositeness and to provide insights into the nature of the near-threshold  $s$ -wave resonances. To achieve these goals, we initially examine near-threshold resonances within the framework of the effective range expansion, considering the principles of the low-energy universality. Subsequently, we put forward a novel probabilistic interpretation of the complex compositeness. Finally, we quantitatively demonstrate that near-threshold  $s$ -wave resonances are not composite dominant, contrary to near-threshold bound states.

*Nature of near-threshold resonances:* Here we summarize the properties of near-threshold resonances in the effective range expansion (ERE) [12]. The single-channel  $s$ -wave scattering amplitude  $f(k)$  with a small momentum  $k$  is expressed only by the scattering length  $a_0$  and effective range  $r_e$ :

$$f(k) = \left[ -\frac{1}{a_0} + \frac{r_e}{2} k^2 + \mathcal{O}(k^4) - ik \right]^{-1}. \quad (1)$$

Discrete eigenstates of the Hamiltonian of the system are expressed by the poles of  $f(k)$  with the analytically continued momentum  $k$  in the complex plane [56–58]. By solving the pole condition  $1/f(k) = 0$ , we obtain two poles  $k^\pm$  as

$$k^\pm = \frac{i}{r_e} \pm \frac{1}{r_e} \sqrt{\frac{2r_e}{a_0} - 1 + i0^+}. \quad (2)$$

Regardless of the signs of  $a_0$  and  $r_e$ , the position of  $k^-$  is always closer to the physical scattering region ( $\text{Re } k \geq 0$  and  $\text{Im } k = 0$ ). From Eq. (2),  $a_0$  and  $r_e$  can be expressed by  $k^\pm$ :

$$a_0 = -\frac{k^+ + k^-}{ik^+k^-}, \quad r_e = \frac{2i}{k^+ + k^-}. \quad (3)$$

In this paper, we consider the system with a negative effective range to realize the resonance solution [12]. Here we note that the  $k^2$  term in Eq. (1) cannot be neglected to describe the resonance pole, because the resonance always appears with the anti-resonance, and the pole condition should be at least quadratic in  $k$ . In this sense, the contribution from  $r_e$  is essential for near-threshold resonances.

Because the resonance pole appears in the  $-\pi/4 \leq \theta_k < 0$  region with  $k^- = |k^-|e^{i\theta_k}$ , we should have  $\text{Re } k^- \geq |\text{Im } k^-|$ . In this case, Eq. (2) gives the following relation:

$$\frac{1}{|r_e|} \sqrt{\frac{2r_e}{a_0} - 1} \geq \frac{1}{|r_e|}, \quad \Rightarrow \quad \frac{r_e}{a_0} \geq 1. \quad (4)$$

From this inequality and the condition of negative  $r_e$ ,  $a_0$  is found to be also negative. We then find that  $|r_e|$  is always larger than  $|a_0|$  for resonances, no matter how large  $|a_0|$  is:

$$r_e \leq a_0 < 0, \quad \Rightarrow \quad |a_0| \leq |r_e|. \quad (5)$$

In other words, the scattering length is not the unique scale for the near-threshold resonance because of the non-negligible effective range, and the low-energy universality does not hold. In fact, we find that not only  $|a_0|$  but also  $|r_e|$  diverge in the  $|k^-| \rightarrow 0$  limit by keeping the relation (5). From this viewpoint, we show that near-threshold resonances are not necessary to be composite dominant in contrast to near-threshold bound states (see supplemental material and a reference [59] therein).

The compositeness of a stable bound state is introduced by expressing its wave function as a superposition of  $|\text{composite}\rangle$  and  $|\text{elementary}\rangle$ . The probability of finding  $|\text{composite}\rangle$  ( $|\text{elementary}\rangle$ ) is defined as the compositeness  $X$  (elementarity  $Z = 1 - X$ ) [6, 14, 26, 31]. The compositeness of near-threshold states is obtained from the weak-binding relation written in terms of  $a_0$  and  $r_e$  [6, 12, 14, 34, 35, 43]:

$$X = \sqrt{\frac{1}{1 - \frac{2r_e}{a_0}}}. \quad (6)$$

For the recent discussion on the finite range correction to Eq. (6), see Refs. [37, 39, 40, 42, 44, 47].

By substituting  $a_0$  and  $r_e$  in Eq. (3) into Eq. (6), we obtain the expression of the compositeness  $X$  in terms of the pole positions [12]. With the relation  $k^+ = -k^{*-}$ , the compositeness of resonances can be expressed only by the argument of the eigenmomentum  $\theta_k$  or by that of the eigenenergy  $\theta_E$ :

$$X = -i \tan \theta_k = -i \tan \left( \frac{1}{2} \theta_E \right). \quad (7)$$

This also shows that the compositeness of near-threshold resonances is pure imaginary [12].

*Interpretation scheme for complex compositeness:* Because the compositeness (7) of resonances is obtained as a complex value, we need to consider its probabilistic interpretation. In the previous works [9–12, 14, 15, 26, 27, 31, 35], some prescriptions were proposed by introducing a fraction associated with the composite component in the resonance. In these proposals, the composite fraction is assigned for any resonances irrespective to their properties. However, a resonance with a large decay width may not be regarded as a physical state in the usual sense due to their unstable nature. It is therefore desirable to introduce a criterion to judge such states to be unphysical within the scheme. Motivated by this idea, we propose an interpretation scheme for the complex compositeness of resonances by referring to Ref. [60]. In Ref. [60], the author discusses the extraction of the resonance contribution from a transition process in nuclear reactions. It is proposed that the intermediate components of the reaction are classified into the following three categories:

- (i) practically certain identification as  $|\text{resonance}\rangle$ ;
- (ii) practically certain identification as not  $|\text{resonance}\rangle$ ;
- (iii) uncertain whether  $|\text{resonance}\rangle$  or not.

The third category is unique and important in Ref. [60]. To extract the resonance contribution from the spectrum, the eigenenergy is not unique due to the finite lifetime and the separation of the resonance from the background is to some extent ambiguous. The category (iii) reflects these ambiguous properties of resonances.

We apply the idea of Ref. [60] to the interpretation of the complex compositeness. In the previous proposals, identification of the internal structure of resonances is classified into two categories; finding  $|\text{composite}\rangle$  or finding  $|\text{elementary}\rangle$ . In this work, we introduce an additional category “uncertain identification”, inspired by the category (iii) mentioned above. Namely, we propose to introduce the probabilities  $\mathcal{X}$ ,  $\mathcal{Y}$ , and  $\mathcal{Z}$ :

$\mathcal{X}$  : probability of certainly finding  $|\text{composite}\rangle$ ;

$\mathcal{Y}$  : probability of uncertain identification;

$\mathcal{Z}$  : probability of certainly finding  $|\text{elementary}\rangle$ .

Now we relate  $\mathcal{X}, \mathcal{Y}, \mathcal{Z}$  with the complex compositeness  $X$ . For the sensible interpretation,  $\mathcal{X}, \mathcal{Y}, \mathcal{Z}$  should be normalized to unity. Furthermore, it is natural to expect  $\mathcal{Y} = 0$  for bound states because  $\mathcal{Y}$  originates in the uncertain nature of resonances. Therefore, we impose the following two conditions so that  $\mathcal{X}, \mathcal{Y}, \mathcal{Z}$  serve as the natural extension of  $X$  and  $Z$  of bound states;

(I) normalization condition:  $\mathcal{X} + \mathcal{Y} + \mathcal{Z} = 1$ ,

(II) bound state condition:  $\mathcal{X} \rightarrow X$ ,  $\mathcal{Z} \rightarrow Z$ , and  $\mathcal{Y} \rightarrow 0$  for bound states with  $0 \leq X \leq 1$ .

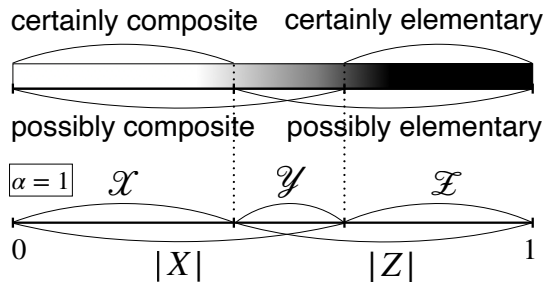


FIG. 1. Schematic illustration of the probabilities  $\mathcal{X}$ ,  $\mathcal{Y}$  and  $\mathcal{Z}$  for  $\alpha = 1$ .

As a prescription consistent with the condition (II), we propose the relation between  $\mathcal{X}$ ,  $\mathcal{Y}$ ,  $\mathcal{Z}$  and  $X$ ,  $Z$ :

$$\mathcal{X} + \alpha\mathcal{Y} = |X|, \quad \mathcal{Z} + \alpha\mathcal{Y} = |Z|. \quad (8)$$

Here  $\alpha > 0$  is a parameter which determines the uncertainty of resonances in the interpretation (see supplemental material).

Let us explain the idea of our proposal (S5). We introduce the fraction of “possibly” composite identification according to Ref. [60] (Fig. S2). This fraction is defined as  $\mathcal{X} + \alpha\mathcal{Y}$  in order to include the probability of the certainly composite identification  $\mathcal{X}$  and a part of the probability of the uncertain identification  $\alpha\mathcal{Y}$ . This expression is reasonable because  $\mathcal{X} + \alpha\mathcal{Y}$  reduces to  $\mathcal{X}$  for bound states ( $\mathcal{Y} = 0$ ) and increases with  $\mathcal{Y}$  for resonances. Because this feature is common to the magnitude of the complex compositeness  $|X|$  which also increases with the uncertain nature of resonances, we further regard the fraction of the possibly composite identification as  $|X|$ . Thus we obtain the relations between  $\mathcal{X}$ ,  $\mathcal{Y}$ ,  $\mathcal{Z}$  and  $X$ ,  $Z$  as in Eq. (S5).

By solving Eq. (S5) for  $\mathcal{X}$ ,  $\mathcal{Y}$ ,  $\mathcal{Z}$  with the normalization condition (I), we obtain the expressions:

$$\mathcal{X} = \frac{(\alpha - 1)|X| - \alpha|Z| + \alpha}{2\alpha - 1}, \quad (9)$$

$$\mathcal{Y} = \frac{|X| + |Z| - 1}{2\alpha - 1}, \quad (10)$$

$$\mathcal{Z} = \frac{(\alpha - 1)|Z| - \alpha|X| + \alpha}{2\alpha - 1}, \quad (11)$$

To proceed, we recall that the probabilities  $\mathcal{X}$ ,  $\mathcal{Y}$ ,  $\mathcal{Z}$  should be positive. We utilize this condition to exclude unphysical states with a large decay width. First,  $\mathcal{Y}$  is guaranteed to be positive by imposing the condition  $\alpha > 1/2$ . Even in this case,  $\mathcal{X}$  and  $\mathcal{Z}$  can be negative, for example, when  $\mathcal{Y}$  is sufficiently large. This case should be associated with large  $|\text{Im } X|$ , indicating that the resonance exhibits highly uncertain nature, based on the definition of the probability  $\mathcal{Y}$ . This suggests that  $\mathcal{X} < 0$  or  $\mathcal{Z} < 0$  occurs for highly uncertain states with a large width for which a sensible interpretation of the internal structure is not possible. We thus adopt a criterion that

TABLE I. Classification of resonances with  $\mathcal{X}$ ,  $\mathcal{Y}$ ,  $\mathcal{Z}$ .

$\mathcal{X} > \mathcal{Y}$ and $\mathcal{X} > \mathcal{Z}$	composite dominant
$\mathcal{X} \geq 0$ and $\mathcal{Z} \geq 0$	$\mathcal{Z} > \mathcal{Y}$ and $\mathcal{Z} > \mathcal{X}$ elementary dominant
	$\mathcal{Y} > \mathcal{X}$ and $\mathcal{Y} > \mathcal{Z}$ uncertain
$\mathcal{X} < 0$ or $\mathcal{Z} < 0$	non-interpretable

the internal structure of resonances with  $\mathcal{X} < 0$  or  $\mathcal{Z} < 0$  cannot be quantified by the compositeness.

In summary, we propose the following classification of resonances (Table I). If either  $\mathcal{X}$  or  $\mathcal{Z}$  is negative, we classify the resonance as a non-interpretable state due to the uncertain nature. Else, if both  $\mathcal{X}$  and  $\mathcal{Z}$  are positive, the internal structure of the resonance can be interpreted in the present scheme. If  $\mathcal{X}$  ( $\mathcal{Z}$ ) is the largest, the state is dominated by the composite (elementary) component. If  $\mathcal{Y}$  is the largest, the nature of the state is uncertain whether elementary or composite. In contrast to the previous proposals, we restrict ourselves to interpret the resonances which share a similar feature with the bound states, and classify the other states as uncertain or non-interpretable.

*Internal structure of near-threshold resonances:* Let us move on to the quantitative analysis of the internal structure of near-threshold  $s$ -wave resonances using  $\mathcal{X}$ ,  $\mathcal{Y}$ ,  $\mathcal{Z}$ . We first discuss the choice of the value of  $\alpha$  by focusing on the eigenenergy  $E$ . It is natural to consider that resonances with a large width  $\Gamma = -2\text{Im } E$  should be classified as non-interpretable. We propose to set the characteristic scale of  $\Gamma$  by the excitation energy  $\text{Re } E$ , and to regard resonances with  $\Gamma > \text{Re } E$  as unphysical and non-interpretable. In other words, the boundary between the physical and non-interpretable states lies on

$$\text{Re } E = -2\text{Im } E, \quad \theta_E = \arctan(-1/2), \quad (12)$$

in the complex  $E$  plane. Here we use the relation (7) between the eigenenergy  $E$  and the compositeness  $X$  in the ERE. In this case,  $X$  is determined by the argument of the eigenenergy and the boundary (12) is straightforwardly implemented. Because  $\mathcal{X}$  and  $\mathcal{Z}$  depend on  $\alpha$  as in Eqs. (9) and (11), the boundary between the non-interpretable and interpretable regions, determined by the values of  $\mathcal{X}$  and  $\mathcal{Z}$ , also depends on  $\alpha$ . From these considerations, we define  $\alpha_0$  as the value of  $\alpha$  with which Eq. (12) gives the boundary.  $\alpha_0$  is then determined by the condition  $\mathcal{X} = 0$  at  $\theta_E$  as

$$\alpha_0 = \frac{\sqrt{5} - 1 + \sqrt{10 - 4\sqrt{5}}}{2} \approx 1.1318. \quad (13)$$

In the following, we set  $\alpha = \alpha_0$ .

Next we numerically evaluate the probabilities  $\mathcal{X}$ ,  $\mathcal{Y}$ ,  $\mathcal{Z}$  of near-threshold  $s$ -wave resonances. Because the compositeness of resonances in the ERE (7) depends only on the argument  $\theta_E$ , we plot  $\mathcal{X}$ ,  $\mathcal{Y}$ ,  $\mathcal{Z}$  in the  $0 < -\theta_E \leq \pi/2$

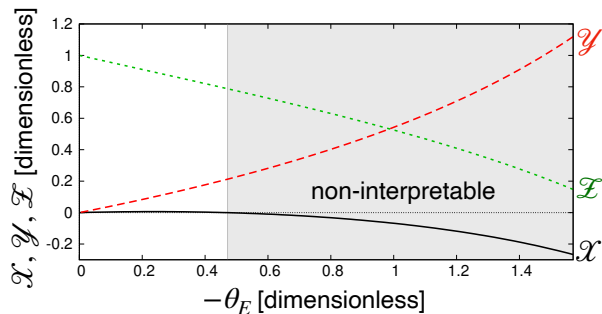


FIG. 2. The probabilities  $\mathcal{X}$ ,  $\mathcal{Y}$ , and  $\mathcal{Z}$  as functions of the argument of the eigenenergy  $-\theta_E$ . The solid line stands for  $\mathcal{X}$ , dashed for  $\mathcal{Y}$ , and dotted for  $\mathcal{Z}$ . The shaded area is the non-interpretatable region determined by the condition (12).

region in Fig. 2. Note that  $\mathcal{X}$  is positive for  $|\theta_E| < |\arctan(-1/2)|$ .

We focus on the interpretable region. In the  $\theta_E \rightarrow 0$  limit,  $\mathcal{X} = \mathcal{Y} = 0$  and  $\mathcal{Z} = 1$  because the complex  $X$  goes to zero as seen in Eq. (7). The pole on the real axis with  $\theta_E \rightarrow 0$  represents the state which does not couple to the scattering states ( $\Gamma = 0$ ). Because the coupling to the scattering states induces the compositeness of the state, it is natural to obtain the completely elementary state with  $\mathcal{Z} = 1$  (e.g. the bare state). The value of  $\mathcal{Z}$  decreases from  $\mathcal{Z} = 1$  with the increase of  $|\theta_E|$ , but the resonance in the interpretable region remains elementary dominant with  $\mathcal{Z} \gtrsim 0.8$ . We therefore conclude that near-threshold resonances with narrow width (small  $|\theta_E|$ ) are elementary dominant in accordance with the model analysis in Ref. [12]. This result shows that the property of near-threshold resonances is completely opposite to near-threshold bound states which are shown to be composite dominant by the low-energy universality [12, 44, 50].

*Comparison with previous works:* Finally, we compare the present results with the previous works by focusing on the elementarity. In Refs. [12, 26, 27, 31, 35], the fraction of the elementary component is defined using the scattering length  $a_0$  and effective range  $r_e$ , or complex compositeness  $X$  as follows:

$$\bar{Z} = 1 - \sqrt{\frac{1}{|1 - 2r_e/a_0|}} \quad (\text{Ref. [12]}), \quad (14)$$

$$\tilde{Z}_{\text{KH}} = \frac{1 - |X| + |1 - X|}{2} \quad (\text{Refs. [26, 31]}), \quad (15)$$

$$\tilde{Z} = \frac{|1 - X|}{|X| + |1 - X|} \quad (\text{Ref. [27]}), \quad (16)$$

$$\bar{Z}_A = 1 - \sqrt{\frac{1}{|1 + |2r_e/a_0|}} \quad (\text{Ref. [35]}). \quad (17)$$

These quantities reduce to the original  $Z$  for bound states. Let us compare these quantities with  $\mathcal{Z}$  for a given set of  $a_0$  and  $r_e$ , where we express  $X$  by  $a_0$  and  $r_e$  using the relation (6). We vary  $1/a_0$  from a positive

value to a sufficiently negative one for a fixed negative  $r_e$  so that a bound state represented by the pole  $k^-$  turns into a virtual state and then into a resonance [12]. Because the fractions of the elementary component (14), (15), (16), (17) and  $\mathcal{Z}$  in Eq. (11) depend only on the ratio of  $r_e$  to  $a_0$ , we plot these quantities as functions of  $-2r_e/a_0$  in Fig. 3 (a).

Before considering resonances, we discuss bound and virtual states. In the  $-2r_e/a_0 > 0$  region where a bound state appears, all the results become identical by definition. In contrast, for a virtual state in the  $-1 < -2r_e/a_0 < 0$  region, the fractions are quite different from each other. The virtual state is interpreted as composite dominant with  $\tilde{Z}_{\text{KH}}$ ,  $\tilde{Z}$ , and  $\bar{Z}_A$ . In particular, with the prescription in Refs. [26, 31],  $\tilde{Z}_{\text{KH}} = 0$  always holds for the virtual state, i.e., completely composite  $\tilde{X}_{\text{KH}} = 1$ . However,  $\tilde{Z}$  and  $\bar{Z}$  are always negative for the virtual state. In our study, the virtual state is classified as non-interpretatable, in agreement with the negative norm of the virtual state which indicates its unphysical nature [61].

A resonance is represented by the pole in the  $-2r_e/a_0 < -2$  region in Fig. 3 (a). The non-shaded area ( $-2r_e/a_0 \lesssim -18$ ) corresponds to the interpretable region where the resonance has a small decay width. To focus on the resonance, in Fig. 3 (b), we plot the fractions as functions of the argument of the eigenenergy  $-\theta_E$  in the whole fourth quadrant ( $0 < -\theta_E \leq \pi/2$ ). We see that all results converge to unity in the  $\theta_E \rightarrow 0$  ( $\Gamma \rightarrow 0$ ) limit. Furthermore, in the interpretable region, all elementarities are larger than 0.7. Hence, it is concluded that near-threshold resonances with a narrow width are elementary dominant with any prescriptions considered here.

*Summary:* In this work, we examine the internal structure of near-threshold  $s$ -wave resonances through quantitative analysis. Initially, we demonstrate that near-threshold  $s$ -wave resonances do not follow the low-energy universality using the ERE. This is attributed to the large negative effective range characteristic of near-threshold resonances.

To analyze the internal structure of resonances, we then introduce a novel probabilistic interpretation scheme for their complex compositeness. The key idea is to incorporate the probability of the uncertain identification in addition to the compositeness and elementarity. Additionally, in this framework, a discernible criterion to exclude unphysical states is inherently embedded. This is our solution related to the first issue.

To address the second issue, using our interpretation scheme, we present quantitative evidence demonstrating that near-threshold resonances with a narrow decay width exhibit elementary dominance. The elementary dominance of resonances holds regardless of the origin, because the compositeness and elementarity are determined within the ERE. This observation can be regarded

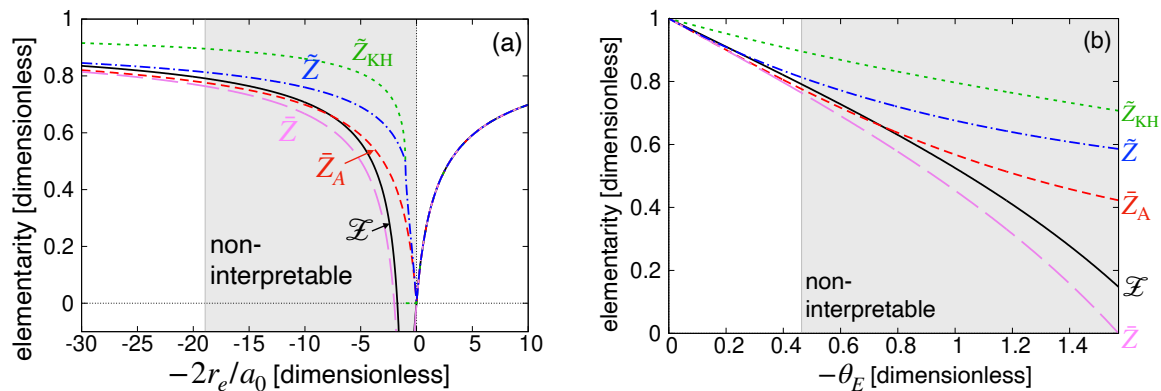


FIG. 3. Fractions of the elementary component as functions of the ratio  $-2r_e/a_0$  [panel (a)], and those as functions of the argument of complex eigenenergy  $-\theta_E$  [panel (b)]. The solid line stands for  $\mathcal{Z}$  in this work, long dashed for  $\bar{\mathcal{Z}}$  in Ref. [12], dotted for  $\tilde{\mathcal{Z}}_{\text{KH}}$  in Refs. [26, 31], dash-dotted for  $\tilde{\mathcal{Z}}$  in Ref. [27], and short dashed for  $\bar{\mathcal{Z}}_A$  in Ref. [35]. The shaded areas are non-interpretable region in this study.

as a kind of the universality inherent to near-threshold resonances. Our analysis underscores the qualitative disparity between near-threshold resonances and shallow bound states, the latter being composite dominant. This indicates that caution must be paid in discussing near-threshold states, as their nature crucially depends on the position relative to the threshold.

This work holds significant implications for the analysis of exotic hadrons. While many near-threshold exotic hadrons are observed [3–5], being near the threshold does not immediately lead to their molecule nature. For example, our findings indicate small  $K^-\Lambda$  compositeness of  $\Xi(1620)$  above the  $K^-\Lambda$  threshold, aligning with the small compositeness  $|g_{K^-\Lambda}^2 dG/dE| = 0.162$  found in Ref. [54].<sup>1</sup> Moreover, our interpretation scheme can be applied to any states with complex compositeness. For instance, we find  $\mathcal{X} = 0.86$ ,  $\mathcal{Y} = 0.01$ , and  $\mathcal{Z} = 0.13$  for  $f_0(980)$  based on the compositeness  $X_{\bar{K}K} = 0.87 - 0.04i$  reported in Ref. [20], indicating the  $\bar{K}K$  molecule dominance of  $f_0(980)$ . In this way, our interpretation scheme for the complex compositeness will be a powerful tool for elucidating the internal structure of exotic hadrons.

This work has been supported in part by the Grants-in-Aid for Scientific Research from JSPS (Grants No. JP23KJ1796, No. JP23H05439, No. JP22K03637, and No. JP18H05402), and by JST, the establishment of university fellowships towards the creation of science technology innovation, Grant No. JPMJFS2139.

\* kinugawa-tomona@ed.tmu.ac.jp

<sup>1</sup> We note that the extension of the present scheme to the coupled-channel case should be considered for more quantitative assessments.

<sup>†</sup> hyodo@tmu.ac.jp

- [1] F. Hoyle, On Nuclear Reactions Occuring in Very Hot Stars. 1. The Synthesis of Elements from Carbon to Nickel, *Astrophys. J. Suppl.* **1**, 121 (1954).
- [2] H. Horiuchi, K. Ikeda, and Y. Suzuki, Molecule-Like Structures in Nuclear System, *Prog. Theor. Suppl.* **52**, 89 (1972).
- [3] F.-K. Guo, C. Hanhart, U.-G. Meißner, Q. Wang, Q. Zhao, and B.-S. Zou, Hadronic molecules, *Rev. Mod. Phys.* **90**, 015004 (2018), [Erratum: *Rev. Mod. Phys.* **94**, 029901 (2022)], arXiv:1705.00141 [hep-ph].
- [4] A. Hosaka, T. Iijima, K. Miyabayashi, Y. Sakai, and S. Yasui, Exotic hadrons with heavy flavors:  $X$ ,  $Y$ ,  $Z$ , and related states, *PTEP* **2016**, 062C01 (2016), arXiv:1603.09229 [hep-ph].
- [5] N. Brambilla, S. Eidelman, C. Hanhart, A. Nefediev, C.-P. Shen, C. E. Thomas, A. Vairo, and C.-Z. Yuan, The  $XYZ$  states: experimental and theoretical status and perspectives, *Phys. Rept.* **873**, 1 (2020), arXiv:1907.07583 [hep-ex].
- [6] S. Weinberg, Evidence That the Deuteron Is Not an Elementary Particle, *Phys. Rev.* **137**, B672 (1965).
- [7] V. Baru, J. Haidenbauer, C. Hanhart, Y. Kalashnikova, and A. E. Kudryavtsev, Evidence that the  $a_0(980)$  and  $f_0(980)$  are not elementary particles, *Phys. Lett. B* **586**, 53 (2004), arXiv:hep-ph/0308129.
- [8] T. Hyodo, D. Jido, and A. Hosaka, Compositeness of dynamically generated states in a chiral unitary approach, *Phys. Rev. C* **85**, 015201 (2012), arXiv:1108.5524 [nucl-th].
- [9] F. Aceti and E. Oset, Wave functions of composite hadron states and relationship to couplings of scattering amplitudes for general partial waves, *Phys. Rev. D* **86**, 014012 (2012), arXiv:1202.4607 [hep-ph].
- [10] C. W. Xiao, F. Aceti, and M. Bayar, The small  $K\pi$  component in the  $K^*$  wave functions, *Eur. Phys. J. A* **49**, 22 (2013), arXiv:1210.7176 [hep-ph].
- [11] F. Aceti, L. R. Dai, L. S. Geng, E. Oset, and Y. Zhang, Meson-baryon components in the states of the baryon decuplet, *Eur. Phys. J. A* **50**, 57 (2014), arXiv:1301.2554 [hep-ph].
- [12] T. Hyodo, Structure of Near-Threshold s-Wave

- Resonances, *Phys. Rev. Lett.* **111**, 132002 (2013), arXiv:1305.1999 [hep-ph].
- [13] G.-Y. Chen, W.-S. Huo, and Q. Zhao, Identifying the structure of near-threshold states from the line shape, *Chin. Phys. C* **39**, 093101 (2015), arXiv:1309.2859 [hep-ph].
- [14] T. Hyodo, Structure and compositeness of hadron resonances, *Int. J. Mod. Phys. A* **28**, 1330045 (2013), arXiv:1310.1176 [hep-ph].
- [15] T. Sekihara and S. Kumano, Determination of compositeness of the  $\Lambda(1405)$  resonance from its radiative decay, *Phys. Rev. C* **89**, 025202 (2014), arXiv:1311.4637 [nucl-th].
- [16] F. Aceti, E. Oset, and L. Roca, Composite nature of the  $\Lambda(1520)$  resonance, *Phys. Rev. C* **90**, 025208 (2014), arXiv:1404.6128 [hep-ph].
- [17] H. Nagahiro and A. Hosaka, Elementarity of composite systems, *Phys. Rev. C* **90**, 065201 (2014), arXiv:1406.3684 [hep-ph].
- [18] T. Hyodo, Hadron mass scaling near the s-wave threshold, *Phys. Rev. C* **90**, 055208 (2014), arXiv:1407.2372 [hep-ph].
- [19] T. Sekihara and S. Kumano, Constraint on  $K\bar{K}$  compositeness of the  $a_0(980)$  and  $f_0(980)$  resonances from their mixing intensity, *Phys. Rev. D* **92**, 034010 (2015), arXiv:1409.2213 [hep-ph].
- [20] T. Sekihara, T. Hyodo, and D. Jido, Comprehensive analysis of the wave function of a hadronic resonance and its compositeness, *PTEP* **2015**, 063D04 (2015), arXiv:1411.2308 [hep-ph].
- [21] A. Martínez Torres, E. Oset, S. Prelovsek, and A. Ramos, Reanalysis of lattice QCD spectra leading to the  $D_{s0}^*(2317)$  and  $D_{s1}^*(2460)$ , *JHEP* **05**, 153, arXiv:1412.1706 [hep-lat].
- [22] F. S. Navarra, M. Nielsen, E. Oset, and T. Sekihara, Testing the molecular nature of  $D_{s0}^*(2317)$  and  $D_0^*(2400)$  in semileptonic  $B_s$  and  $B$  decays, *Phys. Rev. D* **92**, 014031 (2015), arXiv:1501.03422 [hep-ph].
- [23] C. Garcia-Recio, C. Hidalgo-Duque, J. Nieves, L. L. Salcedo, and L. Tolos, Compositeness of the strange, charm, and beauty odd parity  $\Lambda$  states, *Phys. Rev. D* **92**, 034011 (2015), arXiv:1506.04235 [hep-ph].
- [24] U.-G. Meißner and J. A. Oller, Testing the  $\chi_{c1} p$  composite nature of the  $P_c(4450)$ , *Phys. Lett. B* **751**, 59 (2015), arXiv:1507.07478 [hep-ph].
- [25] Z.-H. Guo and J. A. Oller, Probabilistic interpretation of compositeness relation for resonances, *Phys. Rev. D* **93**, 096001 (2016), arXiv:1508.06400 [hep-ph].
- [26] Y. Kamiya and T. Hyodo, Structure of near-threshold quasibound states, *Phys. Rev. C* **93**, 035203 (2016), arXiv:1509.00146 [hep-ph].
- [27] T. Sekihara, T. Arai, J. Yamagata-Sekihara, and S. Yasui, Compositeness of baryonic resonances: Application to the  $\Delta(1232)$ ,  $N(1535)$ , and  $N(1650)$  resonances, *Phys. Rev. C* **93**, 035204 (2016), arXiv:1511.01200 [hep-ph].
- [28] Z.-H. Guo and J. A. Oller, Resonance on top of thresholds: the  $\Lambda_c(2595)^+$  as an extremely fine-tuned state, *Phys. Rev. D* **93**, 054014 (2016), arXiv:1601.00862 [hep-ph].
- [29] J.-X. Lu, H.-X. Chen, Z.-H. Guo, J. Nieves, J.-J. Xie, and L.-S. Geng,  $\Lambda_c(2595)$  resonance as a dynamically generated state: The compositeness condition and the large  $N_c$  evolution, *Phys. Rev. D* **93**, 114028 (2016), arXiv:1603.05388 [hep-ph].
- [30] X.-W. Kang, Z.-H. Guo, and J. A. Oller, General considerations on the nature of  $Z_b(10610)$  and  $Z_b(10650)$  from their pole positions, *Phys. Rev. D* **94**, 014012 (2016), arXiv:1603.05546 [hep-ph].
- [31] Y. Kamiya and T. Hyodo, Generalized weak-binding relations of compositeness in effective field theory, *PTEP* **2017**, 023D02 (2017), arXiv:1607.01899 [hep-ph].
- [32] X.-W. Kang and J. A. Oller, Different pole structures in line shapes of the  $X(3872)$ , *Eur. Phys. J. C* **77**, 399 (2017), arXiv:1612.08420 [hep-ph].
- [33] Y. Tsuchida and T. Hyodo, Compositeness of hadron resonances in finite volume, *Phys. Rev. C* **97**, 055213 (2018), arXiv:1703.02675 [nucl-th].
- [34] J. A. Oller, New results from a number operator interpretation of the compositeness of bound and resonant states, *Annals Phys.* **396**, 429 (2018), arXiv:1710.00991 [hep-ph].
- [35] I. Matuschek, V. Baru, F.-K. Guo, and C. Hanhart, On the nature of near-threshold bound and virtual states, *Eur. Phys. J. A* **57**, 101 (2021), arXiv:2007.05329 [hep-ph].
- [36] A. Esposito, L. Maiani, A. Pilloni, A. D. Polosa, and V. Riquer, From the line shape of the  $X(3872)$  to its structure, *Phys. Rev. D* **105**, L031503 (2022), arXiv:2108.11413 [hep-ph].
- [37] Y. Li, F.-K. Guo, J.-Y. Pang, and J.-J. Wu, Generalization of Weinberg's compositeness relations, *Phys. Rev. D* **105**, L071502 (2022), arXiv:2110.02766 [hep-ph].
- [38] M.-L. Du, V. Baru, X.-K. Dong, A. Filin, F.-K. Guo, C. Hanhart, A. Nefediev, J. Nieves, and Q. Wang, Coupled-channel approach to  $T_{cc}^+$  including three-body effects, *Phys. Rev. D* **105**, 014024 (2022), arXiv:2110.13765 [hep-ph].
- [39] J. Song, L. R. Dai, and E. Oset, How much is the compositeness of a bound state constrained by  $a$  and  $r_0$ ? The role of the interaction range, *Eur. Phys. J. A* **58**, 133 (2022), arXiv:2201.04414 [hep-ph].
- [40] M. Albaladejo and J. Nieves, Compositeness of S-wave weakly-bound states from next-to-leading order Weinberg's relations, *Eur. Phys. J. C* **82**, 724 (2022), arXiv:2203.04864 [hep-ph].
- [41] M. Mikhasenko, Effective-range expansion of the  $T_{cc}^+$  state at the complex  $D^{*+}D^0$  threshold, (2022), arXiv:2203.04622 [hep-ph].
- [42] T. Kinugawa and T. Hyodo, Structure of exotic hadrons by a weak-binding relation with finite-range correction, *Phys. Rev. C* **106**, 015205 (2022), arXiv:2205.08470 [hep-ph].
- [43] U. van Kolck, Weinberg's Compositeness, *Symmetry* **14**, 1884 (2022), arXiv:2209.08432 [hep-ph].
- [44] T. Kinugawa and T. Hyodo, Compositeness of  $T_{cc}$  and  $X(3872)$  by considering decay and coupled-channels effects, *Phys. Rev. C* **109**, 045205 (2024), arXiv:2303.07038 [hep-ph].
- [45] L. R. Dai, L. M. Abreu, A. Feijoo, and E. Oset, The isospin and compositeness of the  $T_{cc}(3875)$  state, *Eur. Phys. J. C* **83**, 983 (2023), arXiv:2304.01870 [hep-ph].
- [46] J. Song, L. R. Dai, and E. Oset, Evolution of compact states to molecular ones with coupled channels: The case of the  $X(3872)$ , (2023), arXiv:2307.02382 [hep-ph].
- [47] Z. Yin and D. Jido, A Possible Reason of Difficulty in the Interpretation of Deuteron Compositeness, (2023), arXiv:2312.13582 [hep-ph].
- [48] E. Braaten and H. W. Hammer, Universality in few-body

- systems with large scattering length, Phys. Rept. **428**, 259 (2006), arXiv:cond-mat/0410417.
- [49] P. Naidon and S. Endo, Efimov Physics: a review, Rept. Prog. Phys. **80**, 056001 (2017), arXiv:1610.09805 [quant-ph].
- [50] C. Hanhart, J. R. Pelaez, and G. Rios, Remarks on pole trajectories for resonances, Phys. Lett. B **739**, 375 (2014), arXiv:1407.7452 [hep-ph].
- [51] H. Sazdjian, The Interplay between Compact and Molecular Structures in Tetraquarks, Symmetry **14**, 515 (2022), arXiv:2202.01081 [hep-ph].
- [52] R. F. Lebed and S. R. Martinez, Diabatic representation of exotic hadrons in the dynamical diquark model, Phys. Rev. D **106**, 074007 (2022), arXiv:2207.01101 [hep-ph].
- [53] C. Hanhart and A. Nefediev, Do near-threshold molecular states mix with neighboring  $Q^-Q$  states?, Phys. Rev. D **106**, 114003 (2022), arXiv:2209.10165 [hep-ph].
- [54] V. M. Sarti, A. Feijoo, I. Vidaña, A. Ramos, F. Giacosa, T. Hyodo, and Y. Kamiya, Constraining the low-energy  $S = -2$  meson-baryon interaction with two-particle correlations, Phys. Rev. D **110**, L011505 (2024), arXiv:2309.08756 [hep-ph].
- [55] T. Kohler, K. Goral, and P. S. Julienne, Production of cold molecules via magnetically tunable Feshbach resonances, Rev. Mod. Phys. **78**, 1311 (2006), arXiv:cond-mat/0601420.
- [56] V. I. Kukulin, V. M. Krasnopol'sky, and J. Horacek, *Theory of Resonances* (Kluwer Academic Publishers, Dordrecht, 1989).
- [57] N. Moiseyev, *Non-Hermitian Quantum Mechanics* (Cambridge University Press, Cambridge, 2011).
- [58] T. Hyodo and M. Niyama, QCD and the strange baryon spectrum, Prog. Part. Nucl. Phys. **120**, 103868 (2021), arXiv:2010.07592 [hep-ph].
- [59] E. J. Bergholtz, J. C. Budich, and F. K. Kunst, Exceptional topology of non-Hermitian systems, Rev. Mod. Phys. **93**, 015005 (2021), arXiv:1912.10048 [cond-mat.mes-hall].
- [60] T. Berggren, On a probabilistic interpretation of expansion coefficients in the non-relativistic quantum theory of resonant states, Phys. Lett. B **33**, 547 (1970).
- [61] E. Braaten, M. Kusunoki, and D. Zhang, Scattering Models for Ultracold Atoms, Annals Phys. **323**, 1770 (2008), arXiv:0709.0499 [cond-mat.other].



— Supplementary Material —

## Compositeness of near-threshold s-wave resonances

Tomona Kinugawa and Tetsuo Hyodo

### EXPRESSION OF THE SCATTERING LENGTH $a_0$ AND EFFECTIVE RANGE $r_e$ BY EIGENMOMENTA

Here we present useful expressions of the scattering length  $a_0$  and effective range  $r_e$  in terms of the eigenmomenta. In the effective range expansion (ERE), two eigenmomenta  $k^\pm$  are determined by  $a_0$  and  $r_e$  as in Eq. (2). Conversely, their expressions in terms of  $k^\pm$  are given by (sum and product of roots) [12]:

$$a_0 = -\frac{k^+ + k^-}{ik^+k^-}, \quad r_e = \frac{2i}{k^+ + k^-}. \quad (\text{S1})$$

The resonance solution is obtained with the condition  $r_e \leq a_0 < 0$ , where  $k^-$  and  $k^+$  correspond to the eigenmomenta of the resonance and anti-resonance, respectively. In this case, complex  $k^\pm$  satisfy the relation  $k^+ = -k^{-*}$ , with which we can rewrite  $a_0$  and  $r_e$  only with the eigenmomentum of the resonance  $k^-$ :

$$a_0 = \frac{2 \operatorname{Im} k^-}{|k^-|^2} = \frac{2 \operatorname{Im} k^-}{(\operatorname{Re} k^-)^2 + (\operatorname{Im} k^-)^2}, \quad r_e = \frac{1}{\operatorname{Im} k^-}. \quad (\text{S2})$$

When  $\operatorname{Re} k^- = -\operatorname{Im} k^-$ ,  $a_0 = r_e$  follows from these equations, corresponding to the equality in Eq. (5). This occurs when the real part of the eigenenergy is zero.  $a_0$  and  $r_e$  can also be expressed by  $|k^-|$  and  $\theta_k$  ( $k^- = |k^-|e^{i\theta_k}$ ) as follows:

$$a_0 = -\frac{2 \sin \theta_k}{|k^-|}, \quad r_e = -\frac{1}{|k^-| \sin \theta_k}. \quad (\text{S3})$$

These equations show that both  $|a_0|$  and  $|r_e|$  diverge in the  $|k^-| \rightarrow 0$  limit in the case of resonance  $-\pi/4 \leq \theta_k < 0$ .

### INTERPRETATION SCHEME

In this section, we give detailed explanation of the interpretation scheme by using  $\mathcal{X}, \mathcal{Y}, \mathcal{Z}$  evaluated from the complex compositeness  $X$  in Eqs. (9), (10), and (11).

To start with, we recall how the compositeness  $X$  of a stable bound state is interpreted as the probability. The wavefunction of the bound state  $|B\rangle$  is expressed by the linear combination  $|B\rangle = \sqrt{X} |\text{composite}\rangle + \sqrt{Z} |\text{elementary}\rangle$ . The compositeness  $X = \langle B | \text{composite} \rangle \langle \text{composite} | B \rangle$  can then be regarded as the expectation value of the projection operator  $|\text{composite}\rangle \langle \text{composite}|$ . Namely,  $X$  is obtained by performing many projective ‘‘measurements’’ of the internal structure of the bound state  $|B\rangle$ . The result of a single measurement gives either 1 (the state is identified as  $|\text{composite}\rangle$ ) or 0 (identified as  $|\text{elementary}\rangle$ ), and the probability of finding 1 in many measurements is the compositeness  $X$ , which takes the value  $0 \leq X \leq 1$ . This is schematically illustrated in Fig. S1 (top row) where we represent the measurement of finding 1 (0) by white (black), and sort out the results from left to right. In this case,  $X$  and  $Z$  correspond to the fractions of white and black regions, respectively.

For an unstable resonance, the wavefunction can be expressed by the linear combination  $|R\rangle = \sqrt{X} |\text{composite}\rangle + \sqrt{Z} |\text{elementary}\rangle$ . Due to the unstable nature of the resonance, the expectation value should be taken with the Gamow vector  $\langle \tilde{R} |$ , leading to the complex valued compositeness  $X = \langle \tilde{R} | \text{composite} \rangle \langle \text{composite} | R \rangle$  [26, 31, 56]. Here we discuss the interpretation of this complex number by considering the results of individual measurement. To obtain the complex value on average, a single measurement would give a complex number, in sharp contrast to the bound state case. We regard that this complex number reflects the uncertainty of the measurement due to the unstable nature of the resonance, as suggested in Ref. [60]. This uncertainty would imply that the result of the measurement cannot be classified as purely composite or purely elementary. Instead, we may regard that the result of the measurement indicates both composite- and elementary-like properties. Given that the result of the measurement of the stable bound state can be classified into either purely composite (white) or purely elementary (black), we may express the degree of composite nature of the resonance state in a single measurement by the grayscale. We sort out the results of the measurements of the internal structure of the resonance according to the composite nature from left to right,



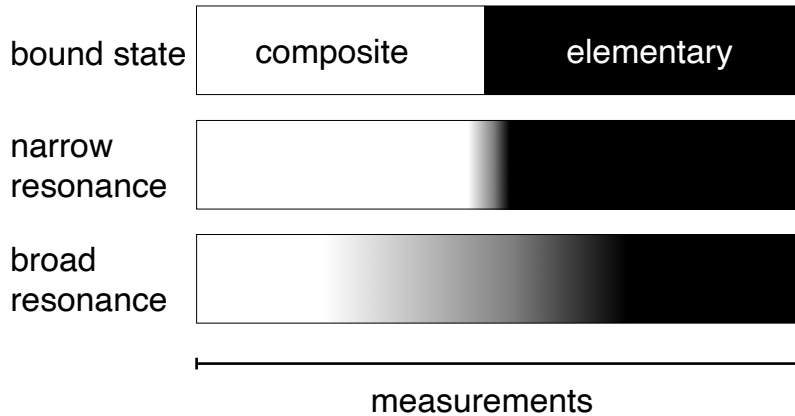


FIG. S1. The schematic illustration of the interpretation of compositeness  $X$  and elementarity  $Z$  of a stable bound state (top row), a narrow resonance (middle row), and a broad resonance (bottom row). The results of the projective measurements of the internal structure of the state are represented by white (composite), black (elementary), and gray (uncertain).

in Fig. S1 (middle and bottom rows). For a narrow resonance (middle row), the uncertainty of the measurement is expected to be small and the most of the measurements can be well classified into composite or elementary. On the other hand, a broad resonance (bottom row) contains substantial gray region, which is uncertain whether composite or elementary. Our task is to assign the probabilities  $\mathcal{X}$ ,  $\mathcal{Y}$ ,  $\mathcal{Z}$  to these results of measurements.

Now let us summarize the notion of “certainly composite” and “possibly composite” probabilities. As we mentioned in the main text, probabilities  $\mathcal{X}$ ,  $\mathcal{Y}$ ,  $\mathcal{Z}$  are introduced as

$\mathcal{X}$  : probability of certainly finding  $|\text{composite}\rangle$ ;

$\mathcal{Y}$  : probability of uncertain identification;

$\mathcal{Z}$  : probability of certainly finding  $|\text{elementary}\rangle$ .

In Fig. S1,  $\mathcal{X}$  and  $\mathcal{Z}$  would correspond to the fractions of certainly white and certainly black regions, respectively. The fraction of the gray region in between would then represent  $\mathcal{Y}$ . We note that the boundary between certainly composite and uncertain identifications is not unique and should be determined by our choice. Namely, we need to determine the boundary to establish the interpretation scheme.

We then introduce the “possibly” composite probability, by including the results which contain a remnant of the composite nature to some extent, in addition to those in  $\mathcal{X}$ . In this case, the possibly composite (elementary) probability should contain the certainly composite (elementary) probability. We also allow that the possibly composite fraction has an overlap with the possibly elementary fraction, when some of the measurements exhibit both the composite and elementary nature. As discussed in Fig. S1, a resonance with large uncertainty contains substantial gray region, indicating the possibly composite probability is large. This shares the common feature with the magnitude of  $|X|$  and  $|Z|$ , which are expected to increase for a resonance with large uncertainty. We thus identify the possibly composite and elementary probabilities as  $|X|$  and  $|Z|$ , respectively:

$|X|$  : probability of possibly finding  $|\text{composite}\rangle$ ;

$|Z|$  : probability of possibly finding  $|\text{elementary}\rangle$ .

Because  $|X| + |Z| \geq 1$  holds from the triangle inequality, the possibly composite and possibly elementary probabilities always overlap with each other, as shown in Fig. S2 (a). Because the possibly composite (elementary) probability should include the certainly composite (elementary) probability, we require

$$|X| > \mathcal{X}, \quad |Z| > \mathcal{Z}. \quad (\text{S4})$$

Because the difference between  $|X|$  (possibly composite) and  $\mathcal{X}$  (certainly composite) reflects the uncertain nature of the resonance, it is expected that the difference increases for a broad resonance and vanishes in the bound state limit. This observation suggests that the difference between  $|X|$  and  $\mathcal{X}$  is proportional to  $\mathcal{Y}$  as

$$|X| = \mathcal{X} + \alpha\mathcal{Y}, \quad |Z| = \mathcal{Z} + \alpha\mathcal{Y}, \quad (\text{S5})$$

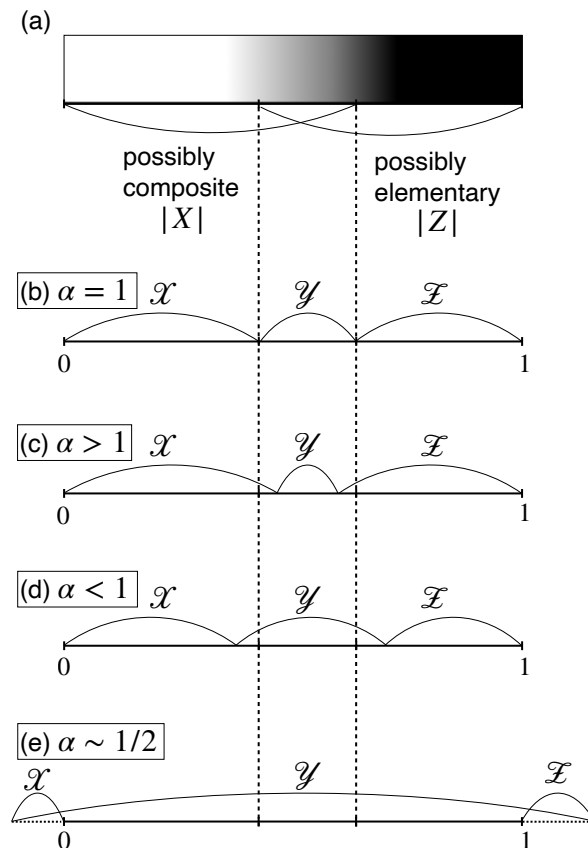


FIG. S2. The schematic illustration of the interpretation of complex compositeness  $X$  and elementarity  $Z$  of an unstable resonance.

by introducing a real parameter  $\alpha > 0$ . We note that this is one of the reasonable choices to relate  $\mathcal{X}, \mathcal{Y}, \mathcal{Z}$  and  $|X|, |Z|$ . With this assignment and the normalization condition  $\mathcal{X} + \mathcal{Y} + \mathcal{Z} = 1$ , we obtain

$$\mathcal{X} = \frac{(\alpha - 1)|X| - \alpha|Z| + \alpha}{2\alpha - 1}, \quad (\text{S6})$$

$$\mathcal{Y} = \frac{|X| + |Z| - 1}{2\alpha - 1}, \quad (\text{S7})$$

$$\mathcal{Z} = \frac{(\alpha - 1)|Z| - \alpha|X| + \alpha}{2\alpha - 1}. \quad (\text{S8})$$

From now on, we discuss the meaning of the parameter  $\alpha$ . From the triangle inequality, the numerator of  $\mathcal{Y}$  in Eq. (10) is positive. Therefore, to obtain positive  $\mathcal{Y}$ , we impose the condition  $\alpha > 1/2$ . From Eq. (S5),  $\alpha\mathcal{Y}$  determines the difference between the possibly composite probability  $|X|$  and the certainly composite probability  $\mathcal{X}$ . Namely,  $\alpha$  determines the weight of  $\mathcal{Y}$  in this assignment. In other words, the magnitude of the certainly composite probability  $\mathcal{X}$  is controlled by  $\alpha$  for a fixed  $X \in \mathbb{C}$ . Alternatively, we may regard that the numerator of  $\mathcal{Y}$  in Eq. (10) ( $|X| + |Z| - 1$ ) corresponds to the overlap of possibly composite and possibly elementary component, and  $\alpha$  in the denominator determines the weight of the overlap in  $\mathcal{Y}$ . In this way, the boundary between  $\mathcal{X}$  and  $\mathcal{Y}$  is determined by the parameter  $\alpha$  (Fig. S2).

Let us discuss the probabilities  $\mathcal{X}, \mathcal{Y}, \mathcal{Z}$  with particular choices of  $\alpha$ . Panels (b), (c), and (d) show the correspondence of the measurements to the probabilities  $\mathcal{X}, \mathcal{Y}, \mathcal{Z}$  with  $\alpha = 1$ ,  $\alpha > 1$ , and  $\alpha < 1$  cases, respectively. In the case with  $\alpha = 1$  [Fig. S2 (b)], the uncertain probability  $\mathcal{Y}$  corresponds to the overlap of the possibly composite and elementary probabilities,  $|X| + |Z| - 1$ , because of  $2\alpha - 1 = 1$ . In other words, the difference between the possibly composite probability ( $|X|$ ) and the certainly composite probability  $\mathcal{X}$  is  $\mathcal{Y}$ . Equivalently,  $\mathcal{Z}$  (certainly elementary) is identified as  $1 - |X|$  (complement of possibly composite fraction).

For  $\alpha > 1$  [Fig. S2 (c)], Eq. (S7) shows that the probability  $\mathcal{Y}$  decreases and therefore  $\mathcal{X}$  and  $\mathcal{Z}$  increase from

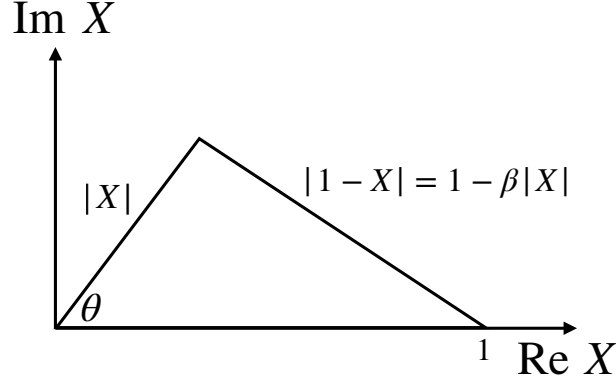


FIG. S3. The geometrical expression of Eq. (S18).

those with  $\alpha = 1$ . This means that we classify larger fraction of the measurements into  $\mathcal{X}$  and  $\mathcal{Z}$  than  $\alpha = 1$ . From Eq. (10), for a larger  $\alpha$ , the probability  $\mathcal{Y}$  becomes smaller. In the  $\alpha \rightarrow \infty$  limit, we obtain

$$\mathcal{X} = \frac{(1 - 1/\alpha)|X| - |Z| + 1}{2 - 1/\alpha} \rightarrow \frac{|X| - |Z| + 1}{2} = \tilde{X}_{\text{KH}}, \quad (\text{S9})$$

$$\mathcal{Z} = \frac{(1 - 1/\alpha)|Z| - |X| + 1}{2 - 1/\alpha} \rightarrow \frac{|Z| - |X| + 1}{2} = \tilde{Z}_{\text{KH}}, \quad (\text{S10})$$

$$\mathcal{Y} = \frac{(|X| + |Z| - 1)/\alpha}{2 - 1/\alpha} \rightarrow 0, \quad (\text{S11})$$

where  $\mathcal{Y}$  vanishes and all the measurements are classified into either certainly composite  $\mathcal{X}$  or certainly elementary  $\mathcal{Z}$ . In addition,  $\mathcal{X}$  and  $\mathcal{Z}$  in the  $\alpha \rightarrow \infty$  limit reduce to  $\tilde{X}_{\text{KH}}$  and  $\tilde{Z}_{\text{KH}}$  proposed in Refs. [26, 31].

If  $\alpha < 1$  [Fig. S2 (d)], the probability  $\mathcal{Y}$  increases from that with  $\alpha = 1$ . This corresponds to assigning uncertain identification  $\mathcal{Y}$  to those classified into  $1 - |X|$  and  $1 - |Z|$  with  $\alpha = 1$ . When  $\alpha \sim 1/2$ ,  $\mathcal{Y}$  can be larger than unity, depending on the value of  $X$ . In this case,  $\mathcal{X}$  and  $\mathcal{Z}$  becomes negative [Fig. S2 (e)] due to the normalization  $\mathcal{X} + \mathcal{Y} + \mathcal{Z} = 1$ . As we discussed in the main text, we regard the state with negative  $\mathcal{X}$  or  $\mathcal{Y}$  as non-interpretable. In the limit  $\alpha \rightarrow 1/2$ , the probabilities  $\mathcal{X}, \mathcal{Y}, \mathcal{Z}$  diverge, corresponding to the non-interpretable assignment for any states except for the bound state satisfying  $0 \leq X \leq 1$ . We will further discuss the interpretation scheme with different  $\alpha$  in the next section.

### $\mathcal{X}, \mathcal{Y}, \mathcal{Z}$ DOMINANT REGIONS

Here, we discuss the classification of the complex compositeness  $X$  into  $\mathcal{X}$ ,  $\mathcal{Y}$ ,  $\mathcal{Z}$  dominant, or non-interpretable regions in the complex  $X$  plane with fixed  $\alpha$ . When the complex compositeness  $X$  is given, the values of  $\mathcal{X}, \mathcal{Y}, \mathcal{Z}$  are calculated from Eqs. (S6), (S7), and (S8). As in Table I, we classify the nature of the resonance according to the values of  $\mathcal{X}, \mathcal{Y}, \mathcal{Z}$ . From Eqs. (S6), (S7), and (S8), the boundary of the  $\mathcal{X}$  dominant region and the  $\mathcal{Z}$  dominant region in the  $X$  plane is determined by

$$\mathcal{X} = \mathcal{Z} \Leftrightarrow (\alpha - 1)|X| - \alpha|1 - X| + \alpha = (\alpha - 1)|1 - X| - \alpha|X| + \alpha, \quad (\text{S12})$$

the boundaries of the  $\mathcal{Y}$  dominant region are

$$\mathcal{X} = \mathcal{Y} \Leftrightarrow (\alpha - 1)|X| - \alpha|1 - X| + \alpha = |X| + |1 - X| - 1, \quad (\text{S13})$$

$$\mathcal{Z} = \mathcal{Y} \Leftrightarrow (\alpha - 1)|1 - X| - \alpha|X| + \alpha = |X| + |1 - X| - 1, \quad (\text{S14})$$

and the boundaries of the non-interpretable region are

$$\mathcal{X} = 0 \Leftrightarrow (\alpha - 1)|X| - \alpha|1 - X| + \alpha = 0, \quad (\text{S15})$$

$$\mathcal{Z} = 0 \Leftrightarrow (\alpha - 1)|1 - X| - \alpha|X| + \alpha = 0. \quad (\text{S16})$$

Because Eq. (S12) gives  $|X| = |1 - X|$ , the boundary between  $\mathcal{X}$  dominant and  $\mathcal{Z}$  dominant regions is obtained as

$$\text{Re } X = \frac{1}{2}, \quad (\text{S17})$$

which is independent of  $\alpha$  and is a natural extension of the real valued compositeness  $X$ . To determine the boundary between  $\mathcal{X}$  dominant and  $\mathcal{Y}$  dominant regions, we rewrite Eq. (S13) as

$$|1 - X| = 1 - \beta|X|, \quad (\text{S18})$$

with

$$\beta = \frac{2 - \alpha}{\alpha + 1}. \quad (\text{S19})$$

Because  $\alpha > 1/2$ ,  $\beta$  is always smaller than unity. In the complex  $X$  plane, we can geometrically express  $X = |X|e^{i\theta}$  as in Fig. S3. Using the cosine formula and Eq. (S18), we obtain

$$\cos \theta = \frac{|X|^2 + 1 - (1 - \beta|X|)^2}{2|X|} \quad (\text{S20})$$

which gives the boundary of  $\mathcal{X} = \mathcal{Y}$  as

$$|X| = \frac{2 \cos \theta - 2\beta}{1 - \beta^2}, \quad (\text{S21})$$

with  $\cos \theta > \beta$ . This boundary can also be expressed by the real and imaginary parts of  $X$ :

$$\text{Re } X = \frac{2 \cos \theta - 2\beta}{1 - \beta^2} \cos \theta, \quad (\text{S22})$$

$$\text{Im } X = \frac{2 \cos \theta - 2\beta}{1 - \beta^2} \sin \theta. \quad (\text{S23})$$

These functions are known as ‘‘limaçon of Pascal’’. From the expressions of  $\mathcal{X}, \mathcal{Y}, \mathcal{Z}$  with  $X, Z$  in Eqs. (S6), (S7), and (S8), we find  $\mathcal{X} \rightarrow \mathcal{Z}$ ,  $\mathcal{Z} \rightarrow \mathcal{X}$ , and  $\mathcal{Y} \rightarrow \mathcal{Y}$  under  $X \leftrightarrow Z$ . This is equivalent to  $X \rightarrow 1 - X$  in the complex  $X$  plane, i.e., the real and imaginary parts of  $X$  change as  $\text{Re } X \rightarrow 1 - \text{Re } X$ , and  $\text{Im } X \rightarrow -\text{Im } X$ , respectively. Therefore, the boundary of  $\mathcal{Z} = \mathcal{Y}$  is obtained from Eqs. (S22) and (S23) as

$$\text{Re } X = 1 - \frac{2 \cos \theta - 2\beta}{1 - \beta^2} \cos \theta, \quad (\text{S24})$$

$$\text{Im } X = -\frac{2 \cos \theta - 2\beta}{1 - \beta^2} \sin \theta. \quad (\text{S25})$$

Next, we consider the boundary between the interpretable and non-interpretable regions in the  $X$  plane. The boundary with  $\mathcal{X} = 0$  is given by Eq. (S15) which can be written as

$$|1 - X| = 1 - \gamma|X|, \quad (\text{S26})$$

with

$$\gamma = \frac{\alpha - 1}{\alpha}. \quad (\text{S27})$$

Following the similar calculation with Eq. (S21) we obtain:

$$|X| = \frac{2 \cos \theta - 2\gamma}{1 - \gamma^2}, \quad (\text{S28})$$

with  $\cos \theta > \gamma$ . Equivalently, we have

$$\text{Re } X = \frac{2 \cos \theta - 2\gamma}{1 - \gamma^2} \cos \theta, \quad (\text{S29})$$

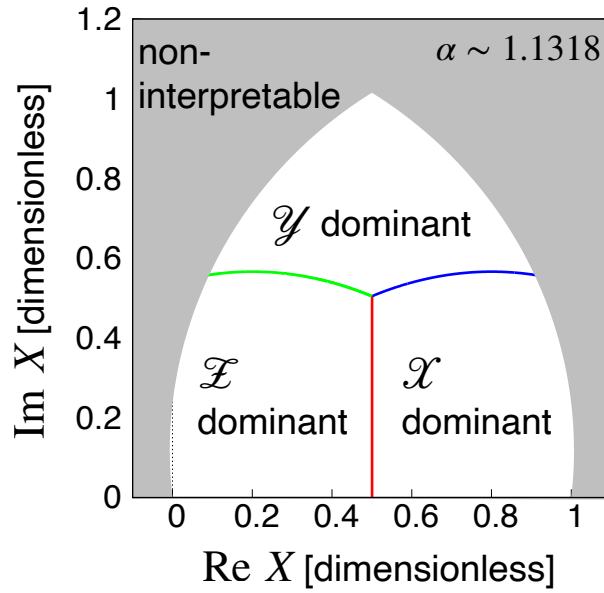


FIG. S4. The  $\mathcal{X}, \mathcal{Y}, \mathcal{Z}$  dominant regions and non-interpretable region (shaded area) in the complex compositeness  $X$  plane with  $\alpha = \alpha_0$ .

$$\text{Im } X = \frac{2 \cos \theta - 2\gamma}{1 - \gamma^2} \sin \theta. \quad (\text{S30})$$

As discussed above, the boundary  $\mathcal{Z} = 0$  is calculated with the replacement  $X \rightarrow 1 - X$ :

$$\text{Re } X = 1 - \frac{2 \cos \theta - 2\gamma}{1 - \gamma^2} \cos \theta, \quad (\text{S31})$$

$$\text{Im } X = -\frac{2 \cos \theta - 2\gamma}{1 - \gamma^2} \sin \theta. \quad (\text{S32})$$

Now we consider the classification of the complex  $X$  plane with Table I by using the boundaries obtained above. To determine the dominant component for a given  $X$ , not all the boundaries are relevant. For instance, the boundary  $\mathcal{X} = \mathcal{Y}$  in the  $\mathcal{Z}$  dominant region is irrelevant, because the boundary classifies the second largest component. In a similar way, the boundaries in the non-interpretable region are also irrelevant. To determine the edge of the boundaries, we calculate  $X$  which gives  $\mathcal{X} = \mathcal{Y} = \mathcal{Z}$ . The condition  $\mathcal{X} = \mathcal{Y} = \mathcal{Z}$  gives

$$|X| = \frac{\alpha + 1}{3}. \quad (\text{S33})$$

From Eq. (S12) we have  $\text{Re } X = 1/2$ , and therefore

$$(\text{Re } X, \text{Im } X) = \left( \frac{1}{2}, \pm \sqrt{\frac{(\alpha + 1)^2}{9} - \frac{1}{4}} \right). \quad (\text{S34})$$

Using  $\text{Re } X = |X| \cos \theta$ , we obtain the corresponding value of the parameter  $\theta$  as

$$\theta = \arccos \left[ \frac{3}{2(1 + \alpha)} \right]. \quad (\text{S35})$$

In Fig. S4, we show the classification of the complex compositeness  $X$  plane into  $\mathcal{X}, \mathcal{Y}, \mathcal{Z}$  dominant or non-interpretable regions for  $\alpha = \alpha_0$  in Eq. (13). Because  $|X|$  and  $|Z| = |1 - X|$  remain unchanged under  $\text{Im } X \rightarrow -\text{Im } X$ , the classification of the complex  $X$  plane is symmetric with respect to the real axis,  $X \rightarrow X^*$ . In other words, it is sufficient to classify the upper half of the complex  $X$  plane. In Fig. S4, on the real axis (bound state case), the states with  $1/2 < X \leq 1$  ( $0 \leq X < 1/2$ ) are composite (elementary) dominant by definition. In the region near the real axis (unstable resonance case), the states with  $\text{Re } X > 1/2$  ( $\text{Re } X < 1/2$ ) are composite (elementary) dominant.

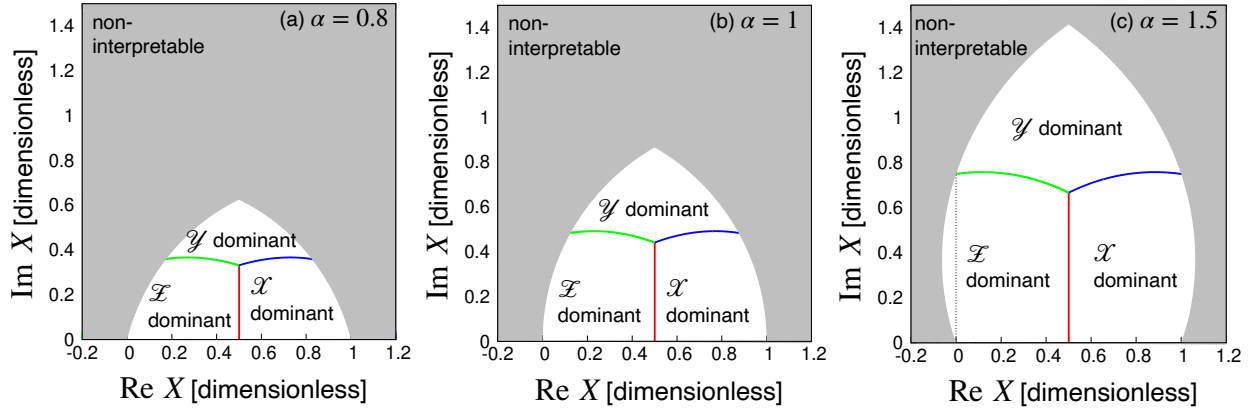


FIG. S5. Same as Fig. S4, but with  $\alpha = 0.8, 1,$  and  $1.5$ .

This feature ensures that our proposal serves as the natural extension of the compositeness of the bound state. For the state with  $0.5 \lesssim \text{Im } X \lesssim 1$ , the uncertain probability  $\mathcal{Y}$  becomes the dominant one. This reflects the idea that  $\mathcal{Y}$  characterizes the uncertain nature of the resonance which is expected to increase for the states with large  $\text{Im } X$ . In the region with  $\text{Im } X \gtrsim 1$ ,  $\text{Re } X \gtrsim 1$ , or  $\text{Re } X \lesssim 0$ , the state is classified as non-interpretable. This is consistent with our expectation that such states are unphysical. To see the  $\alpha$  dependence, we show classifications in the  $X$  plane with  $\alpha = 0.8, 1,$  and  $1.5$  in Fig. S5. The interpretable region with  $\alpha = 1.5$  ( $\alpha = 0.8$ ) is larger (smaller) than that of  $\alpha = 1$ . This tendency is consistent with the fact that whole region becomes interpretable in the  $\alpha \rightarrow \infty$  limit, while only the  $0 \leq X \leq 1$  region is interpretable in the  $\alpha \rightarrow 1/2$  limit. In this way, the parameter  $\alpha$  determines the boundary of the interpretable region.

#### DETERMINATION OF $\alpha_0$

Here we explain the detailed calculation of  $\alpha_0$  in Eq. (13). For the determination of  $\alpha_0$ , we use the ERE where the compositeness of resonances is pure imaginary ( $\text{Re } X = 0$ ) as in Eq. (7). From Figs. S4 and S5, with  $\alpha > 1$ , the state with small  $\text{Im } X$  is interpretable, while the state becomes non-interpretable for large  $\text{Im } X$ . In this case, the boundary of the interpretable region is determined by the condition  $\mathcal{X} = 0$  in Eq. (S15) which depends on  $\alpha$ . We want to determine  $\alpha_0$  so that only narrow width resonances are interpretable and broad resonances are classified as non-interpretable. As seen in Eq. (7), the width of the resonance is related to  $\text{Im } X$  in the ERE. Namely, once we specify the largest width of the interpretable resonances, we find the corresponding value of  $X$  which lies on the boundary of the interpretable region in the complex  $X$  plane. We then determine the relation between  $\alpha$  and  $X$  on the boundary from Eq. (S15) as

$$\alpha(X) = \frac{|X|}{|X| - |1 - X| + 1}. \quad (\text{S36})$$

We adopt the criterion (12) where the states with  $\text{Re } E > \Gamma$  are interpretable. In this case, the value of  $X$  on the boundary is evaluated as (note that  $\sin \theta_E < 0$  and  $\cos \theta_E > 0$ )

$$\begin{aligned} X &= -i \tan \frac{\theta_E}{2} = i \sqrt{\frac{1 - \cos \theta_E}{1 + \cos \theta_E}} = i \frac{1 - \cos \theta_E}{-\sin \theta_E} = i \left[ \frac{1}{\tan \theta_E} - \frac{1}{-\sqrt{\sin^2 \theta_E}} \right] = i \left[ \frac{1}{\tan \theta_E} + \sqrt{\frac{1}{\tan^2 \theta_E} + 1} \right] \\ &= i(-2 + \sqrt{5}). \end{aligned} \quad (\text{S37})$$

By substituting Eq. (S37) into Eq. (S36),  $\alpha_0$  is obtained as:

$$\alpha_0 = \frac{-2 + \sqrt{5}}{\sqrt{5} - 1 - \sqrt{10 - 4\sqrt{5}}} = \frac{\sqrt{5} - 1 + \sqrt{10 - 4\sqrt{5}}}{2}. \quad (\text{S38})$$

## TRAJECTORY OF COMPLEX $X$

In this section, we consider the trajectory of the compositeness  $X$  in the complex  $X$  plane to understand the behavior of the elementarity  $\mathcal{Z}$  in Fig. 3 (a). As shown in Eq. (2), the eigenmomentum  $k^-$  in the ERE is determined by the scattering length  $a_0$  and effective range  $r_e$ . At the same time, the compositeness  $X$  is also calculated by  $a_0$  and  $r_e$  as seen in Eq. (6). From these features of the ERE, we can obtain the trajectory of  $X$  corresponding to that of the pole position by varying  $a_0$  and  $r_e$ . Here, we vary the scattering length from  $1/a_0 = \infty$  to  $-\infty$  with the fixed  $r_e$  being negative. With this variation of  $a_0$ , the pole  $k^-$  moves from the bound state to the resonance through the virtual state and virtual state with width [12].

We show the trajectory of the compositeness  $X$  by the thick solid line in the complex  $X$  plane in Fig. S6. The  $\mathcal{X}, \mathcal{Y}, \mathcal{Z}$  dominant regions in the complex  $X$  plane are also shown with  $\alpha = \alpha_0$ . The triangle, square, circle, cross, and inverted triangle stand for the values of  $X$  whose eigenmomenta are  $k^- = +i\infty$  ( $1/a_0 = +\infty$ ),  $k^- = 0$  ( $1/a_0 = 0$ ),  $k^- = i/r_e$  [ $1/a_0 = 1/(2r_e)$ ],  $k^- = (-1+i)/r_e$  ( $1/a_0 = 1/r_e$ ), and  $k^- = +\infty + i/r_e$  ( $1/a_0 = -\infty$ ), respectively.

At first, we focus on the variation of the compositeness  $X$  from the deep bound state with  $k^- = +i\infty$  (triangle) to the bound state at the threshold with  $k^- = 0$  (square). Because the compositeness of the bound states satisfies  $0 \leq X \leq 1$ , the probability  $\mathcal{X}$  is identical with  $X$  by definition. The trajectory of the compositeness shows that the internal structure of the bound state is completely elementary dominant  $X = \mathcal{X} = 0$  for the deep bound state (triangle), which turns from elementary dominant to composite dominant when the pole moves close to the threshold, and finally the bound state becomes completely composite  $X = \mathcal{X} = 1$  at the threshold (square). This is what the low-energy universality indicates as shown in Refs. [18, 44, 50].

The virtual states without width appears on the negative imaginary axis in the complex  $k$  plane. When the pole position moves from  $k^- = 0$  (square) to  $k^- = i/r_e$  (circle), the corresponding compositeness  $X$  varies in real but  $X > 1$  region. As shown in Fig. S6, the states with  $X > 1$  are non-interpretable. Therefore, we conclude that the virtual states do not have the physical internal structure. In fact, the negative-norm wavefunction of the virtual states cannot be regarded as the physical one [61].

At  $k^- = i/r_e$ , the compositeness  $X$  diverges [12]. If the pole position moves closer to  $k^- = i/r_e + i0^+$ ,  $X$  goes to  $\infty$ . On the other hand,  $X \rightarrow i\infty$  when the pole reaches the divergence point from the complex plane ( $k^- = i/r_e + 0^+$ ). Note that when  $k^- = i/r_e$ , the scattering length is  $1/a_0 = 1/(2r_e)$ , and the other pole also comes to the same position  $k^+ = i/r_e$  as seen in Eq. (2). This means that the two eigenstates with  $k^\pm$  coalesce, and such special point in the parameter space is called the exceptional point [57, 59].

We then consider the virtual states with width whose real part of the eigenmomentum is smaller than the imaginary part,  $\text{Re } k^- < \text{Im } k^-$ . For unstable states, the compositeness  $X$  is calculated as pure imaginary in the ERE as shown in Eq. (7). When the width increases with the variation of the scattering length,  $\text{Im } X$  decreases from  $\infty$  to unity. In this case, the probability  $\mathcal{X}$  is smaller than zero, and virtual states with width are regarded as non-interpretable in this study. In fact, the interpretation of the virtual states with width has not been established yet.

Finally, we discuss the resonances in the  $\text{Re } k^- > \text{Im } k^-$  region. The corresponding trajectory of  $X$  starts from  $\text{Im } X = 1$  (cross), and ends at  $X = 0$  (inverted triangle). If  $\text{Re } E$  is smaller than the width  $\Gamma$ , the resonances are non-interpretable by definition. On the other hand, in  $\text{Re } E \geq \Gamma$  case, the states is  $\mathcal{Z}$  dominant as shown in Fig. S6. In the  $\Gamma \rightarrow 0$  limit, the pole becomes an isolated eigenstate on the real axis of the momentum plane. The compositeness is zero in this case, and the isolated state is interpreted as completely elementary. This is consistent with the expectation from the feature of the resonances with narrow width have a large and negative effective range.

## APPLICATION TO HADRON RESONANCES

As we briefly mentioned in the main text, the interpretation scheme with  $\mathcal{X}, \mathcal{Y}, \mathcal{Z}$  in the present work can be applied to the hadrons whose compositeness  $X$  is given. In Ref. [31], the complex compositeness of  $\Lambda(1405)$ ,  $f_0(980)$ , and  $a_0(980)$  are estimated by the weak-binding relation based on the eigenenergy and the scattering length obtained in various theoretical analyses. In Table I, we summarize the results of  $\mathcal{X}, \mathcal{Y}, \mathcal{Z}$  and the dominant component of each estimation.  $\Lambda(1405)$ ,  $f_0(980)$ , and  $a_0(980)$  are known to be located near the threshold of  $\bar{K}N$ ,  $\bar{K}K$ , and  $\bar{K}K$ , respectively, but the exact pole position depends on the analysis. The difference among the analyses can be regarded as theoretical uncertainty. We classify the nature of the state as a quasibound state (QB) if the real part of the eigenenergy is below the threshold, and as a resonance (R) if it is above. Most of the results in Table I indicate  $\mathcal{X}$  (composite) dominant or  $\mathcal{Z}$  (elementary) dominant, and there is no  $\mathcal{Y}$  (uncertain) dominant classification in the cases examined. Two non-interpretable cases of  $\Lambda(1405)$  shows negative  $\mathcal{Z}$ , but its magnitude is as small as  $|\mathcal{Z}| \lesssim 0.2$ . This means that the compositeness of  $\Lambda(1405)$ ,  $f_0(980)$ , and  $a_0(980)$  is interpretable in the present scheme.



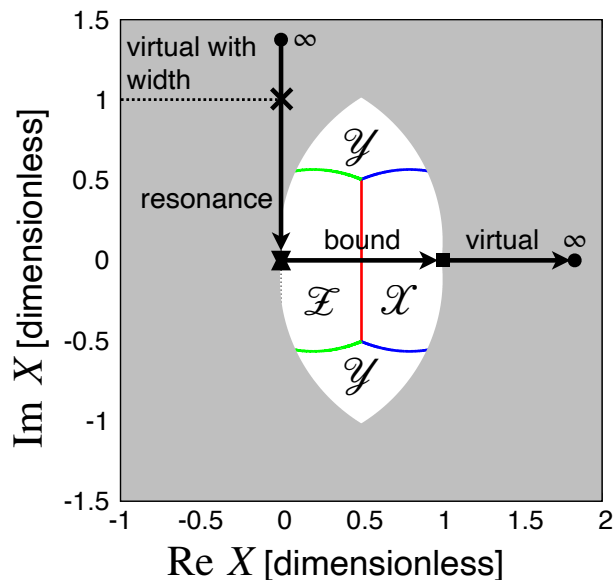


FIG. S6. The plot of the region in the complex plane where the state is  $\mathcal{X}$ ,  $\mathcal{Y}$ , or  $\mathcal{Z}$  dominant, and trajectory of the compositeness  $X$  with the variation of the pole position (solid line). The shaded region stands for the non-interpretable region with  $\alpha = \alpha_0$ . The triangle, square, circle, cross, and inverted triangle represent the compositeness of states whose eigenmomentum are  $k = +\infty i$ ,  $k = 0$ ,  $k = i/r_e$ ,  $k = (1 + i)/r_e$ , and  $k = +\infty$ , respectively.

TABLE I. Interpretation of the compositeness of  $\Lambda(1405)$ ,  $f_0(980)$ , and  $a_0(980)$  in Ref. [31] by  $\mathcal{X}$ ,  $\mathcal{Y}$ ,  $\mathcal{Z}$ .

Hadron (threshold)	$X$	$\mathcal{X}$	$\mathcal{Y}$	$\mathcal{Z}$	Dominant component	Nature	Analysis
$\Lambda(1405)$ ( $\bar{K}N$ )	$1.2 + 0.1i$	0.82	0.34	-0.16	non-interpretable	QB	Set 1 in Table 2
	$0.6 + 0.1i$	0.60	0.02	0.39	$\mathcal{X}$	QB	Set 2 in Table 2
	$0.9 - 0.2i$	0.79	0.12	0.09	$\mathcal{X}$	QB	Set 3 in Table 2
	$0.6 + 0.0i$	0.6	0.0	0.4	$\mathcal{X}$	R	Set 4 in Table 2
	$1.0 + 0.5i$	0.56	0.49	-0.05	non-interpretable	QB	Set 5 in Table 2
$f_0(980)$ ( $\bar{K}K$ )	$0.3 - 0.3i$	0.26	0.15	0.60	$\mathcal{Z}$	R	[42] in Table 5
	$0.3 - 0.1i$	0.30	0.02	0.69	$\mathcal{Z}$	QB	[43] in Table 5
	$0.4 - 0.2i$	0.38	0.06	0.56	$\mathcal{Z}$	QB	[44] in Table 5
	$0.7 - 0.3i$	0.60	0.15	0.26	$\mathcal{X}$	R	[45] in Table 5
	$0.3 - 0.1i$	0.30	0.02	0.69	$\mathcal{Z}$	QB	[46] in Table 5
	$0.9 - 0.2i$	0.79	0.12	0.09	$\mathcal{X}$	R	[47] in Table 5
$a_0(980)$ ( $\bar{K}K$ )	$0.2 - 0.2i$	0.19	0.09	0.73	$\mathcal{Z}$	R	[49] in Table 6
	$0.2 - 0.2i$	0.19	0.09	0.73	$\mathcal{Z}$	R	[50] in Table 6
	$0.8 - 0.4i$	0.59	0.27	0.14	$\mathcal{X}$	R	[51] in Table 6
	$0.1 - 0.2i$	0.09	0.12	0.79	$\mathcal{Z}$	R	[52] in Table 6

In Refs. [18, 44, 50–53], it is shown that the bound state below the threshold is in general composite dominant, while we show in the present work that the resonance above the threshold is elementary dominant. This tendency is reflected in the results of  $\Lambda(1405)$  and  $a_0(980)$  in Table I;  $\Lambda(1405)$  is mostly QB and  $\mathcal{X}$  dominant, while  $a_0(980)$  is R and  $\mathcal{Z}$  dominant. The results of  $f_0(980)$  is somehow scattered, presumably because the pole position is not yet precisely settled. We note that  $\Lambda(1405)$ ,  $f_0(980)$ , and  $a_0(980)$  couples to the lower energy decay channel ( $\pi\Sigma$ ,  $\pi\pi$ , and  $\pi\eta$ , respectively), which may be different from the idealized single-channel situation in the present work. In fact, the decay channel contribution is known to modify the value of the compositeness [44]. For more detailed discussion, we need to estimate the coupled-channel effects on the compositeness in a quantitative manner.